Fast-ion-beam photoelectron spectrometer

K. A. Hanold, C. R. Sherwood, M. C. Garner, and R. E. Continetti
Department of Chemistry and Biochemistry, University of California at San Diego, 9500 Gilman Drive, La Jolla, California 92093-0314

(Received 31 July 1995; accepted for publication 19 September 1995)

A high-collection-efficiency fast-ion-beam photoelectron spectrometer is described. In a straight time-of-flight mode, the spectrometer collects ~1% of the photoelectrons and achieves an energy resolution of $\Delta E/E$ of ~5%. For coincidence experiments requiring greater collection efficiency, a paraboloidal electrostatic mirror is used. The mirror collects ~40% of the photoelectrons while maintaining $\Delta E/E \leqslant 35\%$. In both modes of operation, a time- and position-sensitive electron detector allows conversion of the photoelectron laboratory energy to center-of-mass energy. The fast-ion-beam photoelectron spectrometer is used to prepare mass- and energy-selected neutral molecules which are used in molecular dissociation studies. © *1995 American Institute of Physics.*

I. INTRODUCTION

A new high-collection-efficiency fast-ion-beam photoelectron spectrometer is described. The spectrometer has two modes of operation, a high-resolution mode which uses straight time-of-flight (TOF) and a high-efficiency mode which uses a paraboloidal electrostatic mirror. In both modes of operation, a time- and position-sensitive detector is used to measure the photoelectron laboratory kinetic energy and ejection angle relative to the incident ion beam. This information allows a direct determination of the electron kinetic energy in the center-of-mass (c.m.) frame.

Photodetachment of negative ions is a powerful method for production of mass- and energy-selected neutral molecules and clusters.[1–3] The use of a fast negative-ion beam allows for efficient detection of the neutrals produced by photodetachment, permitting dynamical studies of photodestruction of negative ions[4] and neutral free radicals[2,3] by translational energy spectroscopy. To create energy-selected species by photodetachment, either threshold photodetachment or photodetachment with coincident electron energy analysis can be used. The latter approach is used in the apparatus described in this article.

The difficulty with photodetachment in a fast-ion beam results from the Doppler broadening of the photoelectron kinetic energy spectrum caused by the large ion-beam velocity.[5] Previous high-efficiency ion-beam photoelectron spectrometers have relied on deceleration of the ion beam prior to photodetachment.[6] This is not an option with the present apparatus, as efficient detection of neutral photofragments requires a high laboratory velocity. Thus, to study the dissociation dynamics of mass- and energy-selected neutrals produced by photodetachment, it is necessary to achieve high-resolution photoelectron spectroscopy in a fast-ion beam.

In this article, two approaches to the measurement of photoelectron spectra in a fast-ion beam are described. The first is straight TOF over a short flight path and the second uses an electrostatic mirror to provide very high collection efficiency. The straight TOF setup uses an 80-mm-diam time- and position-sensitive detector with a nominal flight path of 15 cm. This yields a collection efficiency of ~1% and $\Delta E/E$ energy resolution of ~5%. The second approach uses a paraboloidal electrostatic mirror. Paraboloidal electrostatic mirrors have been used previously with thermal velocity molecular beams.[7,8] Coupling the time- and position-sensitive detector with the paraboloidal electrostatic mirror yields a collection efficiency of ~40% and energy resolution of $\leqslant$35%. The time- and position-sensitive detector is required in both modes of operation in order to measure the laboratory kinetic energy and the ejection angle of the electron. Both of these quantities are required to determine the c.m. electron kinetic energy.

II. EXPERIMENTAL METHOD

A schematic of the coupled translational energy and photoelectron spectrometers is shown in Fig. 1. The anion source consists of a pulsed molecular beam crossed by a 1 keV electron beam. After acceleration to 2–7 keV, a TOF mass spectrometer is used to select the anion mass of interest. Similar ion beam lines and photofragment translational energy spectrometers are described in detail elsewhere.[2–4] The fast, mass-selected ion beam is intersected with a pulsed laser beam in an interaction volume ~0.5 mm diam by ~1 mm long. Absorption of a photon can lead to photodetachment of the electron, leaving behind a neutral molecule or neutral photofragments. The photoelectron is energy analyzed using one of the two approaches described below.

In the straight TOF mode of operation, photodetachment occurs 150 mm from the entrance grid of the detector. Photoelectrons ejected along the axis of the electron spectrometer drift region are accepted into the detector. A double-layer mu-metal shield encloses the entire electron spectrometer, reducing the earth's magnetic field to ~1 mG. Residual magnetic fields are eliminated by use of nonmagnetic materials in the construction of this device. Electrostatic patch potentials are reduced by practicing ultrahigh vacuum techniques and coating exposed surfaces with graphite emulsion. The first element of the detector is an acceler-

Downloaded 28 Sep 2007 to 132.239.156.197. Redistribution subject to AIP license or copyright, see http://rsi.aip.org/rsi/copyright.jsp

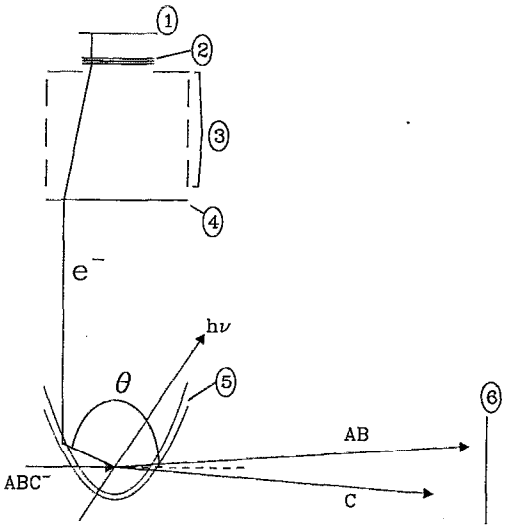

FIG. 1. Schematic of the photoelectron and translational energy release spectrometer. 1=anode, 2=microchannel plates, 3=electrostatic lens, 4=entrance grid, 5=paraboloidal electrostatic mirror, 6=molecular fragment detector. The laboratory ejection angle (θ) is shown.

ating lens which focuses the 80-mm-diam field-free drift region onto the 40-mm-diam microchannel plates. In this lens, photoelectrons are accelerated to ~500 eV where the detection efficiency should be $\geq$50%.[9,10] The microchannel plates are run at high gain to produce a cloud of $\sim 10^7$ secondary electrons. This cloud of secondary electrons impinges on a patterned anode. The centroid of the charge cloud is determined by charge division on a wedge-and-strip anode.[11] This technique has been shown to be capable of <100 μm local resolution, <500 μm global resolution,[12] and <0.5 ns timing resolution.[13] As the wedge-and-strip anode can only record the time and position of one electron per laser shot, the apparatus is run at a repetition rate of 600 Hz with on average $\leq$0.2 event per laser shot.

In the straight TOF mode, the flight path varies from 150 mm for electrons arriving at the middle of the detector to 155 mm for electrons arriving at the edge of the detector. The flight path for each electron is geometrically calculated from the measured position of arrival. The laboratory velocity of the electron is calculated using this flight path and the measured TOF. The c.m. electron velocity (and energy) is then calculated by vectorial subtraction of the known incident ion-beam velocity from the laboratory velocity of the electron.

In the high-collection-efficiency mode of operation, photodetachment occurs at the focus of the paraboloidal electrostatic mirror. The electrons ejected off axis of the electron spectrometer are reflected by the mirror and then travel parallel paths to the detector. The flight path for all electrons reflecting off the mirror is the same. In addition, there is a one-to-one mapping of the electron ejection angle to position of arrival at the detector, allowing determination of the electron ejection angle. Electrons ejected straight toward the detector are mechanically blocked. The detector used in this mode of operation is the same one used for the straight TOF mode.

The mirror consists of two confocal paraboloidal grids. The inner grid and the electron flight tube are held at ground potential. A small reflecting potential (-1 to -5 V) is applied to the outer grid to reflect electrons toward the detector. Confocal grids are used so that each equipotential between the grids is a paraboloid. The inner paraboloidal grid has a focal length of 10.00 mm while the outer paraboloidal grid has a focal length of 10.75 mm. The common focus of the paraboloids is 150 mm from the entrance grid of the detector. This yields a flight path of $\approx$170 mm for all reflected electrons. The diameter of the inner paraboloidal grid is 80 mm, matching the 80-mm-diam entrance grid to the accelerating lens. The grids were made of tungsten mesh (0.001 in. diam, 100 wires/in.), with a transmission of ~80%. The grids were stretched over paraboloidal forms and then clamped by molybdenum rings. The assembly was then plated with copper to fix the paraboloidal shape. Holes (~5 mm diam) for the ion and laser beams were spark etched in the finished grids.

The (x,y) position of the electron at reflection is the same as at the entrance to the detector assuming that the mirror reflects all electrons onto parallel paths. The z coordinate of the electron at reflection can be calculated using the equation of the paraboloids with the assumption that all the electrons reflect at the same depth between the two confocal grids. This assumption ignores a small chromatic aberration in the mirror.[7] A higher energy electron will penetrate deeper into the electric field before being reflected. However, since the grids are separated by ~1 mm, this assumption allows positions to be calculated to <1 mm. Thus, using x_r, y_r, and z_r to designate the position of the electron at reflection,

$$x_r = x_d, \tag{1}$$

$$y_r = y_d, \tag{2}$$

$$z_r = \frac{x_d^2 + y_d^2}{[4(f+d)]} - (f+d), \tag{3}$$

where f is the focal length of the inner grid, x_d and y_d are the positions at the entrance to the detector, and d is the penetration depth of the electron. The polar (θ) and azimuthal (ϕ) ejection angles are determined from the resulting laboratory direction. As in the case of straight TOF, the ejection angles are used to vectorially remove the ion-beam velocity from the electron laboratory velocity to obtain the electron velocity (and energy) in the c.m. frame.

Thus, the contribution of ion-beam velocity to the laboratory velocity of the electron can be removed if the ejection angles of the electron are known. The use of a position-sensitive electron detector makes this possible. For the position of arrival to be meaningful, it is necessary to demonstrate that the measured position at the detector is a one-to-one mapping of the electron ejection angle. The preservation of the electron trajectories in the drift region of the spectrometer was shown by using a thin copper pattern mask at the top of the grids. The image of the pattern was clearly visible on a position map of the detector. The extent to which the mirror can ideally reflect the electrons is best shown by the experimental results in Sec. III B.

Downloaded 28 Sep 2007 to 132.239.156.197. Redistribution subject to AIP license or copyright, see http://rsi.aip.org/rsi/copyright.jsp

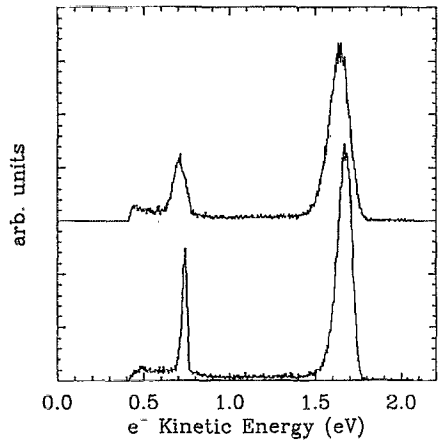

FIG. 2. The laboratory energy spectrum of the photoelectrons from 4 keV I^- at 262 nm is the top histogram. The lower histogram shows the same data after correction for the ion beam velocity.

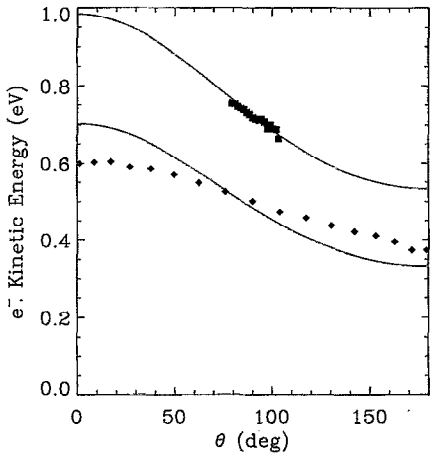

FIG. 3. Laboratory energy of the electrons as a function of laboratory ejection angle. The filled squares are from the straight TOF mode while the filled diamonds are from the mode using the paraboloidal electrostatic mirror. See the text for details.

III. EXPERIMENTAL RESULTS

A. Straight TOF results

Photoelectron energy spectra taken in the straight TOF mode are shown here for I^- at 262 nm and O_2^- at 523 nm. The laboratory photoelectron spectrum of I^- recorded in a 4 keV beam at 262 nm is shown as the upper spectrum in Fig. 2. The higher energy peak in this spectrum corresponds to production of ground state $I(^2P_{3/2})$ and the lower energy peak to spin orbit excited $I(^2P_{1/2})$. In straight TOF mode, the Doppler broadening is not too large due to the small solid angle subtended by the detector. Nonetheless, this kinematic broadening can be removed. The c.m. spectrum for the same data is in the lower spectrum in Fig. 2. The $I(^2P_{1/2})$ peak at 0.7 eV has a full width at half-maximum (FWHM) of 0.04 eV in the c.m. frame, while the peak has 0.10 eV FWHM in the laboratory frame. The increased centroid of the peaks in the lower spectrum is a result of the kinematic correction.

Another measure of the mapping of the electron trajectories is contained in the dependence of the laboratory electron energy on laboratory ejection angle (θ). The Doppler shift due to the ion beam causes electrons ejected into the forward hemisphere (in the direction of the beam) to have higher laboratory energies than those ejected in the backward hemisphere. The filled squares in Fig. 3 show the measured dependence of the photoelectron energy as a function of angle for the 4 keV I^- at 262 mm data. The expected dependence of the electron laboratory velocity is shown as a solid line. Excellent agreement is observed in Fig. 3.

Figure 4 shows photoelectron spectra from a 4 keV beam of O_2^- at 523 nm. The Doppler broadening induced by the parent ion velocity is much greater in this case, as the velocity of O_2^- at 4 keV is twice that of I^-. The spectrometer can still extract high resolution photoelectron energy spectra. The upper histogram shows the laboratory photoelectron spectrum which consists of two broad peaks. The lower histogram shows the same data after correcting for the ion beam velocity. The vibrational progressions in the $O_2(^3\Sigma_g^-)$ and $O_2(^1\Delta_g)$ states are clearly visible. This spectrum compares well with those previously reported in the literature.[14–16] In both O_2^- and I^-, the resolution ($\Delta E/E$ at 0.06 eV=5%) is limited by the laser pulse width (6 ns FWHM).

These data show that the kinematic effects of the ion-beam velocity can be successfully removed from photoelectron spectra recorded in a fast-ion beam. It should be noted here that the collection efficiency of the straight TOF mode is about 1%, which is ~100 times larger than the acceptance of conventional ion-beam TOF electron spectrometers.[17,18]

B. Paraboloidal mirror results

The paraboloidal electrostatic mirror allows a much larger range of ejection angles to be accepted by the electron detector. The solid angle subtended by the detector increases from ~1% of 4π sr for straight TOF measurements to ~80% of 4π sr when using the mirror. The grids are 80% transparent and each electron must pass through the inner paraboloidal grid twice. The entrance grid to the detector is also 80% transmitting. This implies that ~50% of the electrons are lost

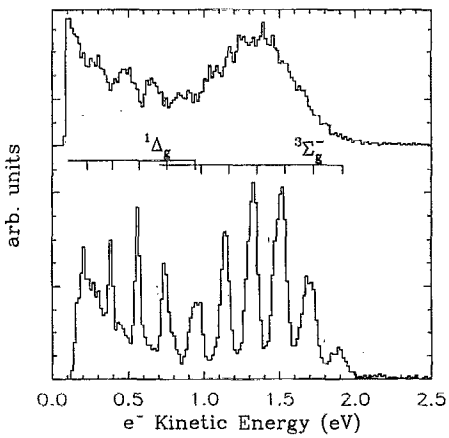

FIG. 4. The laboratory energy spectrum of the photoelectrons from 4 keV O_2^- at 523 nm is the top histogram. The lower histogram shows the same data after correction for the ion beam velocity.

Downloaded 28 Sep 2007 to 132.239.156.197. Redistribution subject to AIP license or copyright, see http://rsi.aip.org/rsi/copyright.jsp

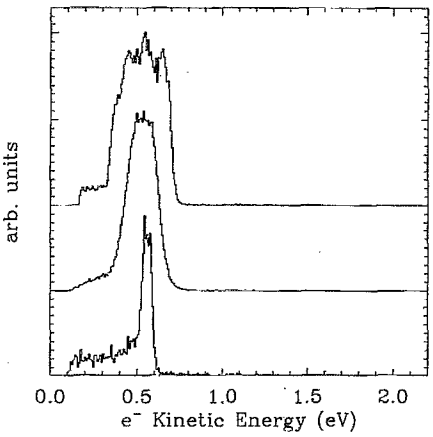

FIG. 5. The photoelectron energy spectra using a paraboloidal electrostatic mirror. The laboratory energy of the photoelectron from 4 keV I^- at 349 nm is the top histogram. The middle histograms shows the same data after correction for the ion-beam velocity. The lower histogram shows the corrected data from only the forward third of the detector.

due to collisions with grids. A quantitative measure of the collection efficiency was not made, although it was estimated to be ~40%.

The dependence of the laboratory energy on ejection angle for 4 keV I^- at 349 nm taken using the mirror is shown in Fig. 3 as filled diamonds. The expected dependence of the electron laboratory velocity is shown as a solid line. Good qualitative agreement is observed in Fig. 3, indicating that the mirror is generally preserving the 1:1 mapping of ejection angle to position. The discrepancies indicate that the mirror is not working perfectly.

The laboratory photoelectron energy spectrum of a 4 keV beam of I^- at 349 nm is shown as the top histogram in the upper frame of Fig. 5. The same data after position correction are shown as the middle spectrum in the same figure. The resolution is improved, however, the resolution is significantly reduced compared to straight TOF. The bottom histogram shows the data from the forward third of the detector after the position correction was applied. This part of the detector had the best resolution ($\Delta E/E$ at 0.5 eV=13%) while using the entire detector gave worse resolution ($\Delta E/E$ at 0.5 eV=35%). The improved performance of the forward third of the detector may indicate that the higher laboratory energy forward-ejected photoelectrons are more nearly optically reflected.

IV. DISCUSSION

High-resolution photoelectron spectra were obtained in the straight TOF mode, with ~1% collection efficiency. The resolution of the present measurements are limited by the laser pulse width of 6 ns FWHM. These results can be improved by decreasing the laser pulse width. Using time-to-amplitude converter techniques with a microchannel-plate-based detector can easily provide <500 ps timing resolution. Implementation of a picosecond laser system should allow us to reduce the flight path and increase the solid angle to 6% for straight TOF. The performance of the acceleration lens and the size of the laser/ion beam interaction volume may ultimately be limiting factors in this case.

The reduced resolution of the high-efficiency mode using the paraboloidal electrostatic mirror can be ascribed to several factors. Field penetration through the holes in the grids for the laser and ion beams may play a role. In addition, it is recognized that grid-based electrostatic lenses have shortcomings as imaging devices due to the field penetration through each grid opening.[8,19] Trevor *et al.* have discussed the effects of the chromatic aberration.[7] Shirley and coworkers performed numerical calculations that showed slight focusing effects for the electrons emerging from the mirror.[20] The size and location of the laser–ion beam interaction volume relative to the focal point of the confocal grids may also cause nonideal reflection. All of these factors probably contribute to the observed resolution. Reduction of the flight path by a factor of 2 and use of a 100 ps light source should allow improvements in both the mirror collection efficiency and resolution.

Photoelectron spectroscopy using straight TOF kinetic energy analysis with a large solid angle in a fast-ion beam has been demonstrated. Good energy resolution was obtained despite the high ion velocity. We have also demonstrated the use of a paraboloidal electrostatic mirror in a fast-ion-beam environment as a means of greatly increasing the electron collection efficiency while paying only a small price in energy resolution. The high electron collection efficiency of the mirror makes coincidence measurements of the photoelectron and neutral fragments possible. We have recently performed a photoelectron–neutral–neutral coincidence measurement of the translational energy partitioning in the dissociative photodetachment of O_4^- ($O_4^- + h\nu \rightarrow O_2 + O_2 + e^-$).[21]

ACKNOWLEDGMENTS

This work was supported by the National Science Foundation. R.E.C. thanks Dr. J. A. Syage for helpful discussions. R.E.C. gratefully acknowledges the Camille and Henry Dreyfus Foundation for a New Faculty Award and the David and Lucile Packard Foundation for a 1994 Fellowship in Science and Engineering.

[1] S. Suzuki, T. Wakabayashi, H. Matsuma, H. Shiromaru, C. Kittaka, and Y. Achiba, Chem. Phys. Lett. **182**, 12 (1991).
[2] R. E. Continetti, D. R. Cyr, R. B. Metz, and D. M. Neumark, Chem. Phys. Lett. **182**, 406 (1991).
[3] R. E. Continetti, D. R. Cyr, D. L. Osborn, D. J. Leahy, and D. M. Neumark, J. Chem. Phys. **99**, 2616 (1993).
[4] C. R. Sherwood, M. C. Garner, K. A. Hanold, K. M. Strong, and R. E. Continetti, J. Chem. Phys. **102**, 6949 (1995).
[5] H. Hotop and W. C. Lineberger, J. Phys. Chem. Ref. Data **14**, 731 (1985).
[6] O. Cheshnovsky, S. H. Young, C. C. Pettiette, M. J. Craycraft, and R. E. Smalley, Rev. Sci. Instrum. **58**, 2131 (1987).
[7] D. J. Trevor, L. D. Van Woerkom, and R. R. Freeman, Rev. Sci. Instrum. **60**, 1051 (1989).
[8] J. Steadman and J. A. Syage, Rev. Sci. Instrum. **64**, 3094 (1993).
[9] A. Müller, N. Djurić, G. H. Dunn, and D. S. Belić, Rev. Sci. Instrum. **57**, 349 (1986).
[10] The stated collection efficiencies do not include this detection efficiency.

Downloaded 28 Sep 2007 to 132.239.156.197. Redistribution subject to AIP license or copyright, see http://rsi.aip.org/rsi/copyright.jsp

Thus the actual detection efficiency for the straight TOF mode is ~0.5% and for the mode using the mirror is ~20%.
[11] C. Martin, P. Jelinsky, M. Lampton, R. F. Malina, and H. O. Anger, Rev. Sci. Instrum. **52**, 1067 (1981).
[12] O. H. W. Siegmund, R. F. Malina, K. Coburn, and D. Werthimer, IEEE Trans. Nucl. Sci. **NS-31**, 776 (1984).
[13] A. Belkacem, A. Faibis, E. P. Kanter, W. Koenig, R. E. Mitchell, Z. Vager, and B. J. Zabransky, Rev. Sci. Instrum. **61**, 945 (1990).
[14] R. J. Celotta, R. A. Bennet, J. L. Hall, M. W. Siegel, and J. Levine, Phys. Rev. A **6**, 634 (1972).
[15] M. J. Travers, D. C. Cowles, and G. B. Ellison, Chem. Phys. Lett. **16**, 449 (1989).
[16] M. J. Deluca, C. C. Han, and M. A. Johnson, J. Chem. Phys. **93**, 268 (1990).
[17] L. A. Posey, M. J. Deluca, and M. A. Johnson, Chem. Phys. Lett. **131**, 170 (1986).
[18] R. B. Metz, A. Weaver, S. E. Bradforth, T. N. Kitsopoulos, and D. N. Neumark, J. Phys. Chem. **94**, 1377 (1990).
[19] O. Klemperer and M. F. Barnett, *Electron Optics* (Cambridge University Press, Cambridge, 1971).
[20] G. Liu, J. J. Barton, C. C. Bahr, and D. A. Shirley, Nucl. Instrum. Methods A **246**, 504 (1986).
[21] K. A. Hanold, C. R. Sherwood, and R. E. Continetti, J. Chem. Phys. (in press).

Downloaded 28 Sep 2007 to 132.236.180.11. Redistribution subject to AIP license or copyright, see http://rsi.aip.org/rsi/copyright.jsp